TISSUE ENGINEERING: Part A
Volume 21, Numbers 1 and 2, 2015

DOI: 10.1089/ten.tea.2014.0008

Tensile Forces Applied on a Cell-Embedded Three-Dimensional Scaffold Can Direct Early Differentiation of Embryonic Stem Cells Toward the Mesoderm Germ Layer

Dekel Dado-Rosenfeld, MSc, Itai Tzchori, PhD, Amir Fine, MSc,
Limor Chen-Konak, PhD, and Shulamit Levenberg, PhD

Mechanical forces play an important role in the initial stages of embryo development; yet, the influence of forces, particularly of tensile forces, on embryonic stem cell differentiation is still unknown. The effects of tensile forces on mouse embryonic stem cell (mESC) differentiation within a three-dimensional (3D) environment were examined using an advanced bioreactor system. Uniaxial static or dynamic stretch was applied on cell-embedded collagen constructs. Six-day-long cyclic stretching of the seeded constructs led to a fourfold increase in Brachyury (*BRACH-T*) expression, associated with the primitive streak phase in gastrulation, confirmed also by immunofluorescence staining. Further examination of gene expression characteristic of mESC differentiation and pluripotency, under the same conditions, revealed changes mostly related to mesodermal processes. Additionally, downregulation of genes related to pluripotency and stemness was observed. Cyclic stretching of the 3D constructs resulted in actin fiber alignment parallel to the stretching direction. *BRACH-T* expression decreased under cyclic stretching with addition of myosin II inhibitor. No significant changes in gene expression were observed when mESCs were first differentiated in the form of embryoid bodies and then exposed to cyclic stretching, suggesting that forces primarily influence nondifferentiated cells. Understanding the effects of forces on stem cell differentiation provides a means of controlling their differentiation for later use in regenerative medicine applications and sheds light on their involvement in embryogenesis.

Introduction

Embryonic stem cells (ESCs) can be indefinitely maintained in an undifferentiated state but also bear the potential to differentiate to most cell types.[1,2] Several techniques have been applied to induce ESC differentiation *in vitro*, including culture in monolayers on extracellular matrix (ECM) proteins and formation of three-dimensional (3D) cell aggregates, termed embryoid bodies (EBs) that can be further differentiated upon administration of specific factors[3–5] or culture within microfluidics chambers.[6,7] Newly emerging techniques use 3D polymeric scaffolds, allowing for stem cell organization into multicellular tissues.[8–12] While numerous studies have shed light on the elements governing ESC differentiation,[13–15] some dominant regulating factors, including mechanical elements, remain elusive.

It has been firmly established that mechanical forces play a dominant role in transformation of the embryo from a group of undifferentiated cells into the three primary germ layers, namely, the ectoderm, mesoderm, and endoderm.[16–19] Recent studies have shown that mechanical manipulations, in the form of forces, substrate geometry, and stiffness, can influence the behavior and differentiation of stem cells.[20–25] More specifically, ESCs have been shown to respond to the mechanical properties of their substrates, as manifested by channeled differentiation toward the mesoderm germ layer on stiffer scaffolds.[26] Additionally, manipulation of the magnitude and duration of shear stress was shown to influence ESC differentiation.[27,28]

This study evaluated the capacity of mechanical strain to provide signaling cues influential on the early stages of mouse embryonic stem cell (mESC) differentiation. We hypothesized that mechanical forces in the form of tensile stretching can direct ESC differentiation. Specific emphasis was placed on the impact of such manipulations on formation of the mesoderm germ layer, which later gives rise to cells naturally exposed to mechanical forces within the body.

To this end, mESCs were cultured within highly porous 3D collagen scaffolds, which were mechanically manipulated within an advanced computer-controlled bioreactor system. Cell differentiation under the applied mechanical forces was examined through gene and protein analysis.

Department of Biomedical Engineering, Technion–Israel Institute of Technology, Haifa, Israel.

Additionally, the contribution of forces in the differentiation process was examined through inhibition of the nonmuscle myosin II, responsible for force transmission to the cell.

The ability to control ESC differentiation through mechanical manipulations can facilitate *in vitro* fabrication of multicellular tissues. With such added depth of appreciation of the involvement of forces in differentiation, this study can pave the way for extensive *in vitro* use of controlled ESC culture and differentiation within 3D constructs under a fine-tuned regimen of external forces.

Materials and Methods

Cell culture

Mouse Nestin-GFP-expressing ESCs[29] were grown on mitomycin-C-treated, neomycin-resistant, primary mouse embryonic fibroblasts (MEFs; Chemicon, Temecula, CA, Millipore Corporate, Billerica, MA) in Dulbecco's modified Eagle's medium (DMEM; Gibco, Carlsbad, CA) supplemented with 15% fetal bovine serum (HyClone Laboratories, Logan, UT), 2 mM L-glutamine, 1 mM sodium pyruvate, 0.1 mM β-mercaptoethanol, 0.1 mM nonessential amino acids, 50 U/mL penicillin/50 μg/mL streptomycin (Gibco), and 1000 U/mL leukemia inhibitory factor (Chemicon). After removing the cells from their MEF feeder layer, they were grown on porous Helistat absorbable deep flexor (Achilles) tendon collagen hemostatic sponges ($5 \times 5\ mm^2$; Integra Life Sciences, Plainsboro, NJ) in DMEM supplemented with 15% knockout serum, 0.1 mM β-mercaptoethanol, 0.1 mM nonessential amino acids, 1 mM sodium pyruvate, 50 U/mL penicillin, and 50 μg/mL streptomycin.

In some experiments, cells were first grown in the form of EBs before being seeded on the scaffold. EBs were formed by placing a cell suspension on a low-adherence, 10-cm Petri dish (Ein-Shemer, Shomron, Israel) immediately after the cells had been detached from their feeder layer. The dish was then incubated in a CO_2 incubator until they were seeded on the scaffold.

Collagen scaffold characterization

Scaffold morphology with and without cells was examined using a scanning electron microscope (SEM) (Quanta 200; FEI, Eindhoven, The Netherlands). The scaffold samples were gold-coated using a Polaron gold coater operated at 0.1 Torr and 20 mA, and were observed under a vacuum of 1.7×10^{-6} Torr, 10–20 kV, and an emission current of 100 μA. Cell-embedded scaffolds were prepared as follows: scaffolds were immersed in 2.5% glutaraldehyde in 0.1 M cacodylate buffer (Sigma-Aldrich, St. Louis, MO) for 5 min, followed by dehydration with ethanol gradients of 70%, 85%, 95%, and 100% for 5 min each. Scaffolds were then immersed in hexamethyldisilazane (Sigma-Aldrich) for 5 min and air dried at room temperature.

The mechanical properties of hydrated scaffolds (ramp) were examined using the Biodynamic test instrument (BD, @Electroforce, Bose, Eden Prairie, MN), by means of a uniaxial tensile test with a strain rate of 0.01 mm/min until failure was reached. To measure the mechanical properties of cell-embedded scaffold, constructs were grown within the BD system for 4 days and then subjected to the same ramp protocol. Strain was calculated as change in length divided by initial length. Stress was defined as the measured force divided by the cross-sectional area. Stiffness was assessed according to the slope of the linear part of the stress–strain curve. Ultimate tensile strength (UTS) is the maximum stress in the stress–strain curve.

Mechanical stimulation

The BD test instrument was used to apply tensile forces on cell-seeded 3D constructs. This system allows for mechanical manipulations of 3D biological samples within a sterile environment and within an incubator. Uniaxial stretch was applied to a rectangular-shaped scaffold held between the system's grips. The protocols included static stretching, to obtain constant displacement on the construct, and oscillatory displacement, with an amplitude of 1.5 mm ($\sim$30% strain) and a frequency of 0.3 Hz. The control samples were grown in each experiment and included constructs held on one grip inside the system, under the same culture condition, with minimum forces on the construct.

Quantitative polymerase chain reaction

Following each experiment, scaffolds were maintained in RNA-later (Qiagen, Valencia, CA) at 4°C until homogenization. RNA was purified from the dispersed cells using the RNeasy mini kit (Qiagen). RNA concentrations were quantified using the NanoDrop® spectrophotometer and the isolated RNA was reverse-transcribed using the High-capacity cDNA Reverse Transcription Kit (Applied Biosystems, Chicago, IL). cDNA was amplified with the Step One Plus Real-time PCR System (Applied Biosystems), according to standard protocols.[26] Gene expression levels were normalized to those of the *GAPDH* gene and the minimal cycle threshold was determined for each sample.

To monitor mESC differentiation and pluripotency, a broader range of genes was further examined using the TaqMan® Array Custom Micro Fluidic Card (TaqMan® mouse Stem Cell Pluripotency Array). The TaqMan array card was loaded with cDNA samples (1 μg) mixed with the TaqMan® Universal PCR Master Mix. The Applied Biosystems 7900HT Fast Real-Time PCR System was used for gene amplification and SDS Software v3 (Applied Biosystems) was used for gene analysis, all according to the manufacturer's instructions. All gene values were normalized to the *GAPDH* gene expression levels.

Immunohistochemistry

Scaffolds were fixed with 4% paraformaldehyde for 20 min. For frozen-embedded sections, scaffolds were maintained overnight in a 30% sucrose solution and then embedded within optimal cutting temperature compound (Tissue-Tek®, Torrance, CA). Immunofluorescence or hematoxylin and eosin (H&E) staining was performed on transverse sections (5 μm) placed on slides. For immunostaining, sections were permeabilized with a 0.5% Tween solution (Sigma-Aldrich) for 20 min, at room temperature. Sections were then washed with phosphate-buffered saline (PBS) and immersed for 30 min in blocking solution (0.5% Probumin® bovine serum albumin; Millipore Corporate). Immunofluorescence staining was performed by incubating samples with goat anti-brachyury antibody (0.1 mg/μL; R&D, Minneapolis, MN), overnight at 4°C,

and then with Cy3-conjugated anti-goat IgG (1:100; Jackson Immunoresearch Laboratory, West Grove, PA) for 30 min, at room temperature. 4′,6-Diamidino-2-phenylindole (DAPI; Sigma-Aldrich) was used for nuclear counterstaining.

Whole-construct staining of actin fibers was performed on scaffolds permeabilized with 0.3% Triton X-100 (Bio Lab Ltd., Jerusalem, Israel), for 10 min at room temperature. Scaffolds were then washed in PBS, and immersed overnight in blocking serum (10% fetal bovine serum and 0.1% Triton X-100) at 4°C. Phalloidin-TRITC (0.5 μg/mL; Sigma-Aldrich) was added for 20 min with DAPI for nuclear counterstaining.

All images were captured using a Leica™ TCS LSI superzoom macroconfocal microscope.

Image analysis

Protein expression was quantified from immunofluorescence staining using MATLAB (The Mathworks, Natick, MA). Double-blinded images were taken at several sections of each type of sample, under the various mechanical conditions. For each image, the total number of cells was estimated by the extent of DAPI staining and the BRACH-positive cells were estimated by the extent of the Cy3 signal. The percent of BRACH-positive cells versus the total number of cells is presented.

Myosin II inhibition

Blebbistatin (50 μM; Sigma-Aldrich) was added to the culture medium for the entire duration of the experiments in order to inhibit nonmuscle myosin II under cyclic stretching.

Statistical analysis

All results are shown as mean ± standard error. When comparing two groups, Student's *t*-test was used. Significant results were considered with probability value ≤ 0.05.

Median results of four experiments are shown for the TaqMan array card.

Results

We aimed to examine the influence of mechanical manipulation of 3D mESC-embedded scaffolds on the early stages of cell differentiation. Single-cell mESC samples were cultured within a collagen scaffold mounted within the Biodynamic test system and subjected to either static or cyclic stretching. A control group was grown under the same conditions within the system, but without additional external forces. An illustration of the experimental protocol is presented on Figure 1.

Collagen scaffold characterization

The properties of the collagen scaffold were examined to confirm its suitability for the planned mechanical experiments. SEM-based analysis demonstrated that the scaffold featured an interconnective fibrillar structure with pores of varying sizes (50–200 μm), supportive of cell infiltration (Fig. 2A). The internal structure remained stable at 4 days postseeding. Cells covered the scaffold and filled its pores; some small pores were fully concealed by the cells. Cells residing within the pores generated groups of cells in the form of EBs, which is preferred for cell differentiation (Supplementary Fig. S1; Supplementary Data are available online at www.liebertpub.com/tea).

Using the BD system, scaffold elastic modulus was measured as ~21 kPa, with a UTS of 12 kPa, and strain at UTS of about 80% (Fig. 2B, C). The observed porosity and stiffness, along with high strain at UTS, enable mechanical manipulations of the scaffold without risk of rupture, obviating the need for an additional supportive matrix. One cycle of the stress–strain curve derived from the cyclic stretching protocol demonstrated a hysteresis loop, suggestive of viscoelastic scaffold behavior. A slight decrease in scaffold stiffness (elastic modulus of 13 kPa) and strength (UTS of 5 kPa) was observed at 4 days postseeding (Fig. 2C). This decrease is likely due to cell-driven degradation of the scaffold and yields a stiffness and strength of the same order as acellular scaffolds, demonstrating its ability to resist the mechanical manipulation and to transmit the forces to the cells.

H&E staining of scaffold with cells 6 days postseeding showed that, under all tested conditions, cells were more clustered and seemed to form EB structures within the scaffold pores (Fig. 2D). Following cyclic stretching, the groups of cells were more dispersed throughout the scaffold and scaffold fibers were less dense and more aligned.

mESC differentiation into the three germ layers

To examine the impact of the different mechanical conditions on mESC differentiation, representative genes of each germ layer were examined (summarized in Fig. 3A and Supplementary Table S1). After 2 days of cyclic stretching of 3D scaffolds embedded with undifferentiated cell cultures, *BRACH-T*, a gene associated with primitive streak of early gastrulation phase, expression was upregulated when compared with control scaffolds (Supplementary Fig. S2). The temporal significance of mechanical manipulations on differentiation response was further examined by monitoring gene expression of cells first grown for 4 days as EBs and then mechanically manipulated for additional 3 days after being seeded onto the scaffold. This setup involves application of the mechanical forces after the cells have already exited their nondifferentiated state. Under these conditions, no significant changes in gene expression profiles were observed following stretching (Fig. 3B), suggesting that mechanical stresses are primarily sensed by undifferentiated cells.

Following a 6-day-long exposure to mechanical manipulations, no significant changes in gene expression were observed following static stretching, when compared with control samples (Fig. 3C). However, upon application of cyclic stretching, the most significant changes were observed in *BRACH-T* expression, which was upregulated fourfold. In parallel, immunohistochemical analysis of scaffold sections demonstrated an increased number of cells expressing BRACH following cyclic stretching, when compared with both static stretching and control stress conditions (Fig. 4), demonstrating compatibility between mRNA and protein levels.

We next evaluated the impact of a 6-day cyclic stretching regimen applied to mESC-embedded collagen scaffolds on germ-layer-specific differentiation, using a TaqMan Array

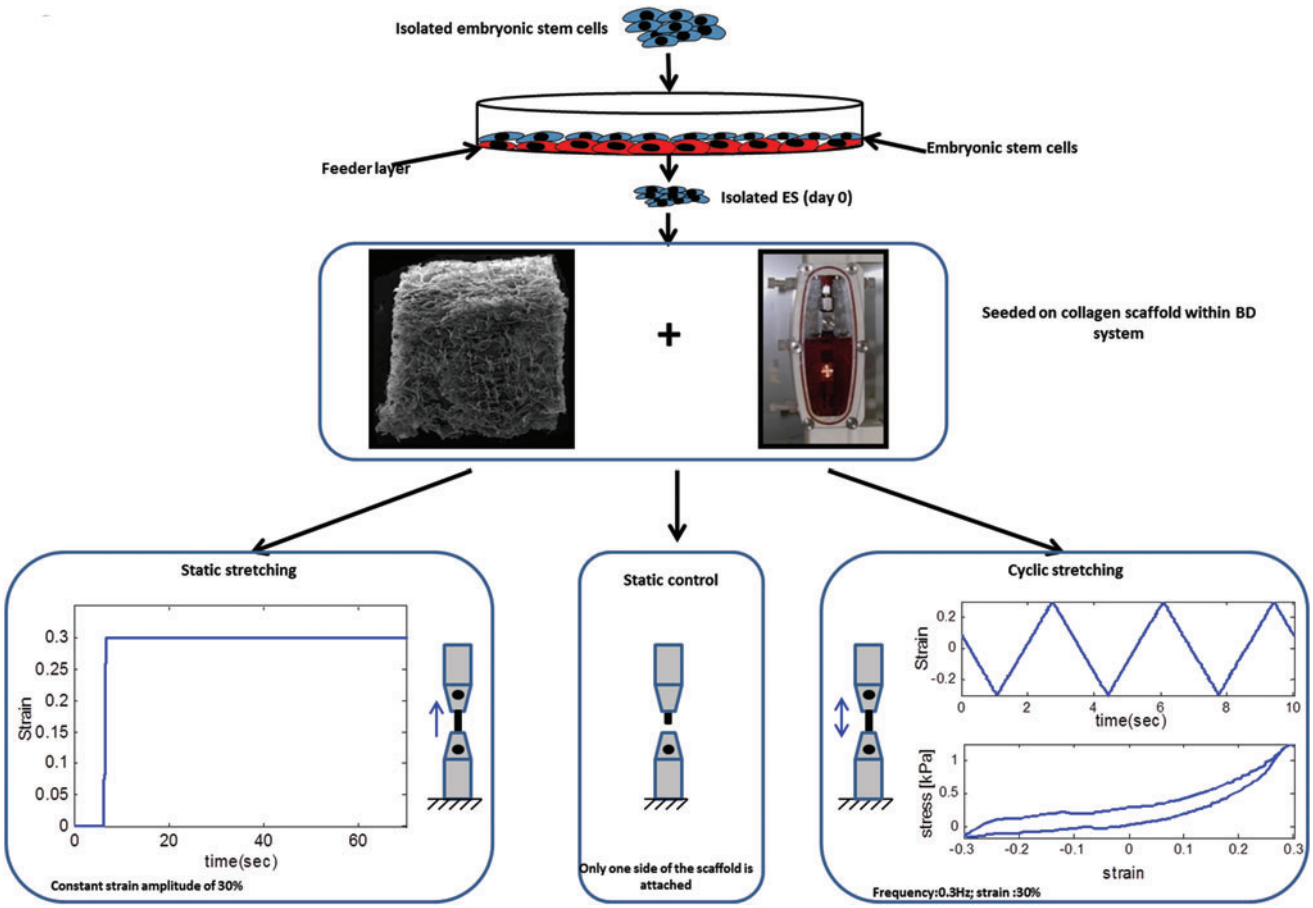

FIG. 1. Mechanical manipulations of collagen scaffolds seeded with mouse embryonic stem cells (mESCs). Experiment protocols included are as follows: static stretching—constant strain with an amplitude of 30%; static control—scaffolds were attached to one side of the system chamber and were exposed to the same experiment conditions but without additional external forces; and cyclic stretching—frequency of 0.3 Hz with a strain amplitude of 30%. Color images available online at www.liebertpub.com/tea

Custom Micro Fluidic Card. The list of examined genes is presented in Supplementary Figure S3 indicating the role of the significant upregulated genes. Genes upregulated or downregulated by more than 20%, in at least three of four experiments, are presented and were classified as either representative of one of the three germ layers (Fig. 5A), or as pluripotency- and stemness-associated genes (Fig. 5B). A group of mesoderm-specific genes was highly affected (upregulated or downregulated) by cyclic stretching. For example, *Actc1*, a gene associated with cardiomyocytes, a mesoderm-derived cell type,[30] was upregulated 1.75-fold, while *col2a1*, associated with chondrogenesis, was upregulated 1.4-fold.[31] Extensive upregulation (11.64-fold) in the expression of *Myf5*, which plays a key role both in regulating muscle differentiation and in the early stages of embryogenesis, was observed.[32] *BRACH-T* upregulation detected by the real-time polymerase chain reaction (PCR) analysis was further corroborated by the results of the microarray analysis, which measured a 2.63-fold upregulation in its expression levels.

At the same time, most genes representing the ectoderm and endoderm layers were downregulated, as were stemness and pluripotency genes. The resulting gene profile (Fig. 5C) correlated with those described, implies for processes such as vasculogenesis, cell differentiation, migration, morphology, proliferation, and mesoderm development (Fig. 5D).

Inhibition of myosin II decreases mesodermal differentiation under cyclic forces

Inhibition of myosin II prevents the transmission of applied external forces to the cells.[33] It has been shown that myosin II plays an important role in regulation of actomyosin–microtubule crosstalk, through its mediation of cell tension and contractility.[34] We aimed to examine whether myosin II plays a role in transmission of cyclic forces applied on the cells and to assess its influence on cell differentiation. Following exposure to cyclic stretching, actin fiber alignment was observed and cells were more dispersed, when compared with control conditions (Fig 6A, B). In contrast, in the presence of blebbistatin (50 μM), punctate actin staining replaced the previously observed fiber-like structures (Fig. 6C). Gene expression analysis of mESC-embedded scaffolds exposed to cyclic stretching in the presence of blebbistatin demonstrated downregulated expression of all genes, with the mesoderm-associated *BRACH-T* and *Flk1* genes undergoing the highest degree of downregulation.

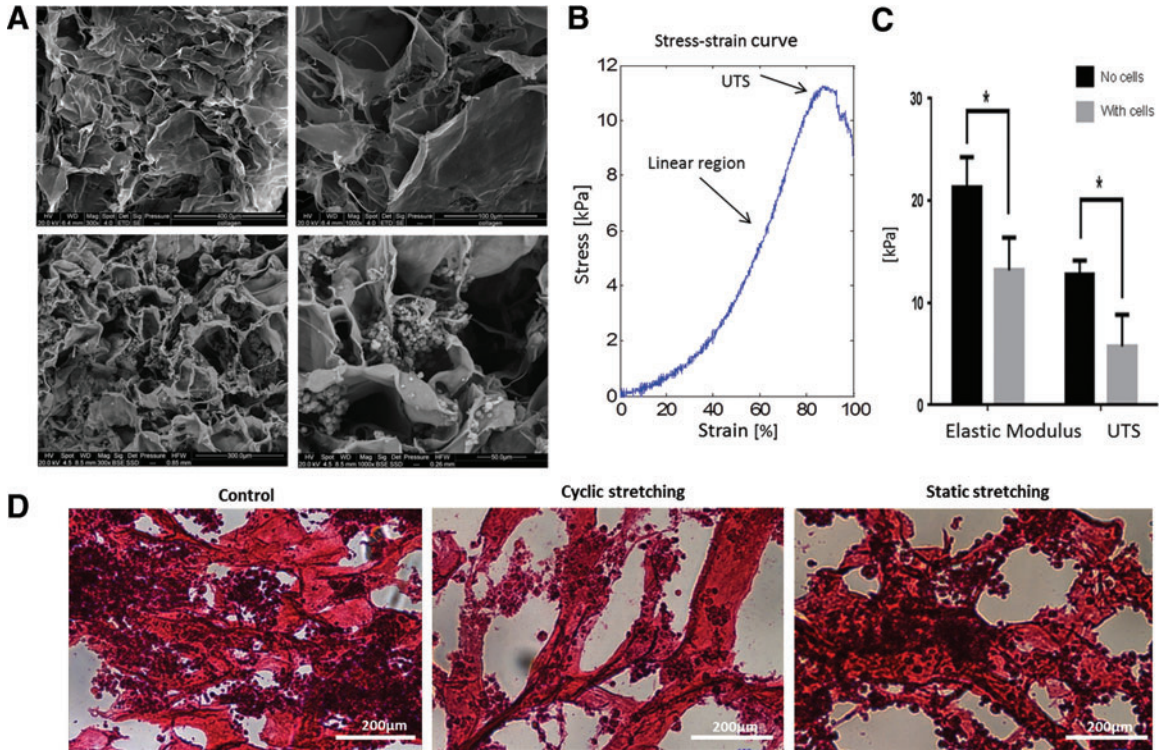

FIG. 2. Suitability of collagen scaffold for mESC growth. **(A)** Representative scanning electron microscopy micrographs of a Helistat collagen scaffold. Upper: scaffold with no cells at two magnifications. Lower: scaffold with cells at two magnifications. **(B)** A typical stress–strain curve of the Helistat collagen scaffold. Elastic modulus was determined as the linear region of the curve and the ultimate tensile strength (UTS) was defined as the maximum stress in the curve. **(C)** Elastic modulus and UTS as measured with the BD system for scaffold only ($n=3$) and scaffold with cells ($n=2$). Mean ± standard deviation is presented. **(D)** Hematoxylin and eosin staining of mESC-embedded collagen scaffold after 6 days of exposure to one of the three examined conditions: control, static stretching, and cyclic stretching. (*$p \leq 0.05$). Color images available online at www.liebertpub.com/tea

A

Gene	Attributed germ layer
Brachyury (BRACH-T)	Primitive streak
Flk1	Mesoderm
Nestin (Nes)	Ectoderm
Pax6	Ectoderm
Sox17	Endoderm

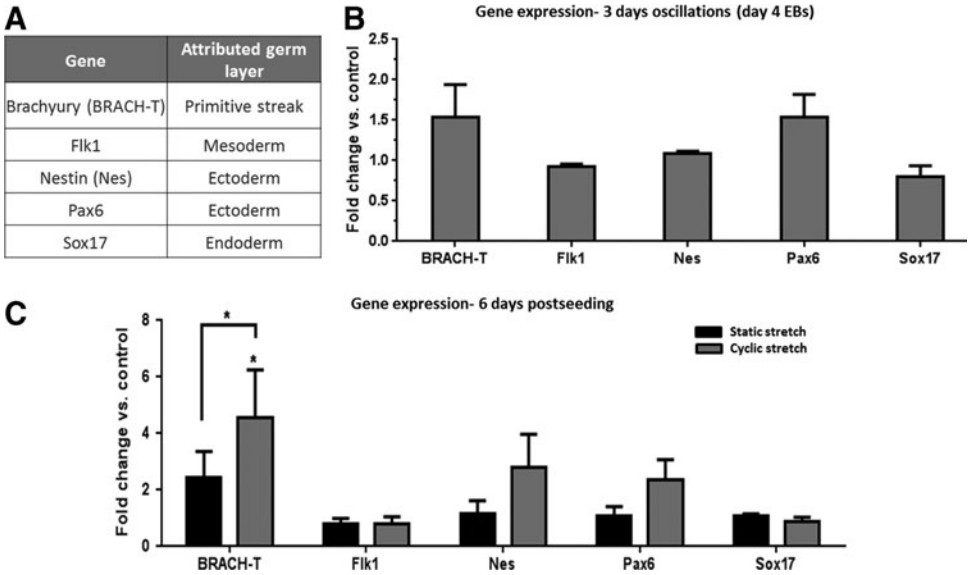

FIG. 3. Real-time polymerase chain reaction (PCR) analysis of gene markers of the three germ layers. Cells were seeded on collagen scaffolds and exposed to external forces: **(A)** A list of genes and their associated germ layer. **(B)** Fold change versus control in gene expression after 3 days of cyclic stretching of 4-day-old embryoid bodies (EBs) seeded on scaffolds. **(C)** Fold change versus control in gene expression after 6 days of cyclic stretching of mESC-embedded scaffolds. Mechanical manipulation results were normalized to those of the trail-matched static control. Means ± standard error are presented, where significant differences are marked with asterisks ($p \leq 0.05$).

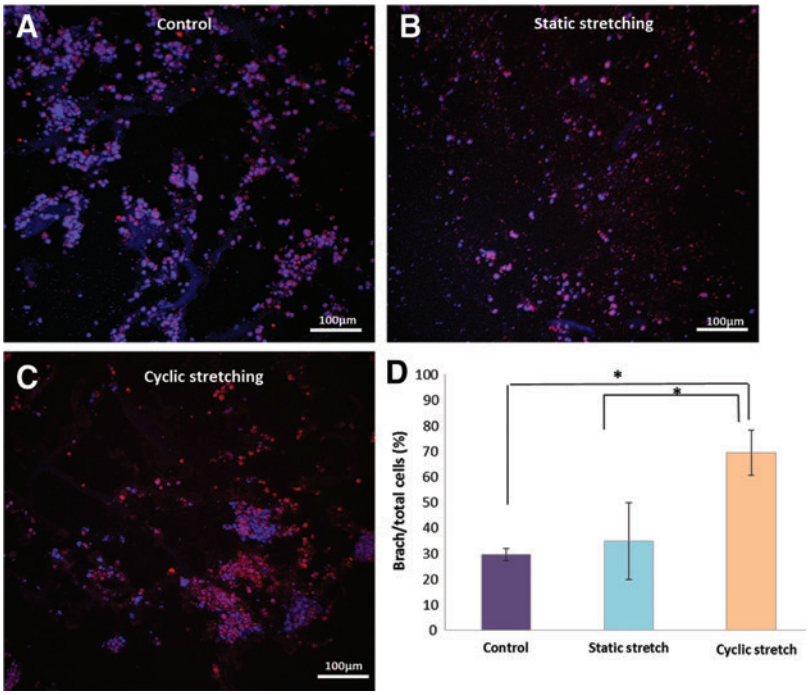

FIG. 4. Bry immunofluorescence staining in mESC-embedded collagen scaffolds following mechanical stress. Bry staining of mESCs grown on collagen scaffolds for 6 days under various mechanical conditions: **(A)** control, **(B)** static stretch, or **(C)** cyclic stretching. **(D)** Image analysis quantification of immunofluorescence staining for Bry versus total number of cells. Means ± standard error are presented ($n = 5$–8). Significant differences of groups are marked with asterisks ($p \leq 0.05$). Color images available online at www.liebertpub.com/tea

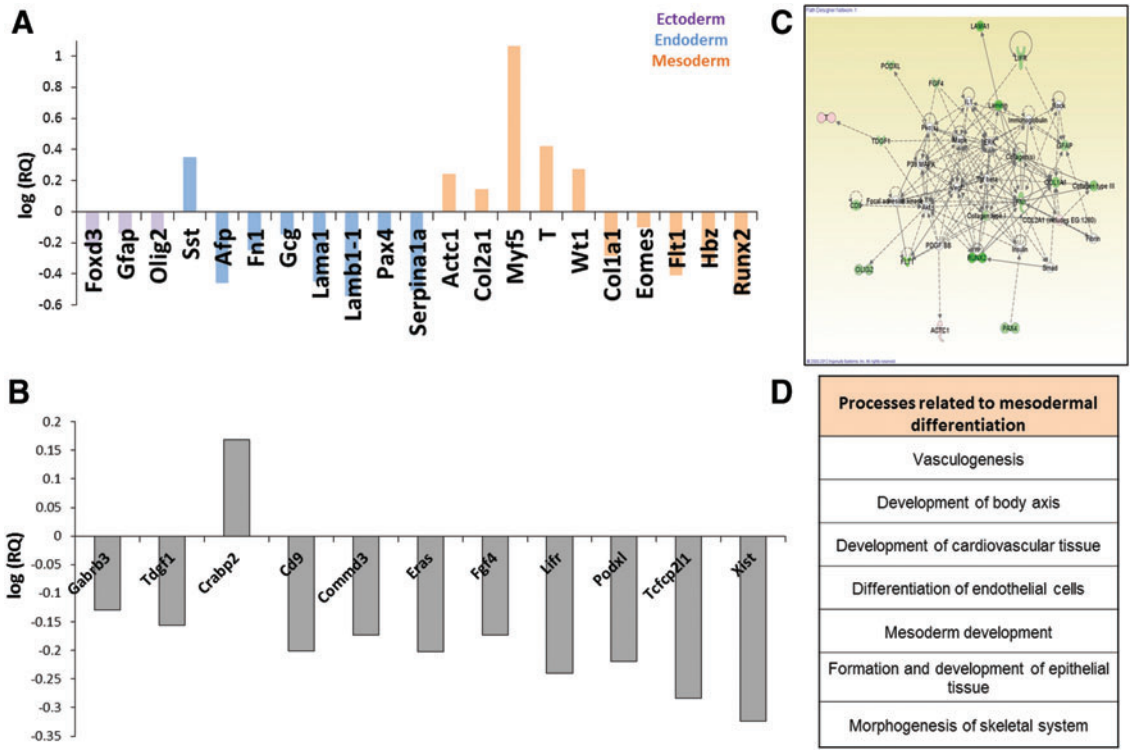

FIG. 5. Altered gene expression in mESC-embedded collagen scaffolds following exposure to cyclic stretching, as determined using a TaqMan® Array Custom Micro Fluidic Card. **(A)** Fold change (log scale) in expression of genes representing the three germ layers upregulated or downregulated by >20% in at least three of four experiments. **(B)** Fold change (log scale) in expression of genes associated with cell stemness or pluripotency upregulated or downregulated by >20% in at least three of four experiments. **(C)** A gene enrichment map of all the genes in the array that were downregulated or upregulated. **(D)** Cellular processes related to the resulting gene expression profile. Processes related to mesodermal differentiation are presented. Color images available online at www.liebertpub.com/tea

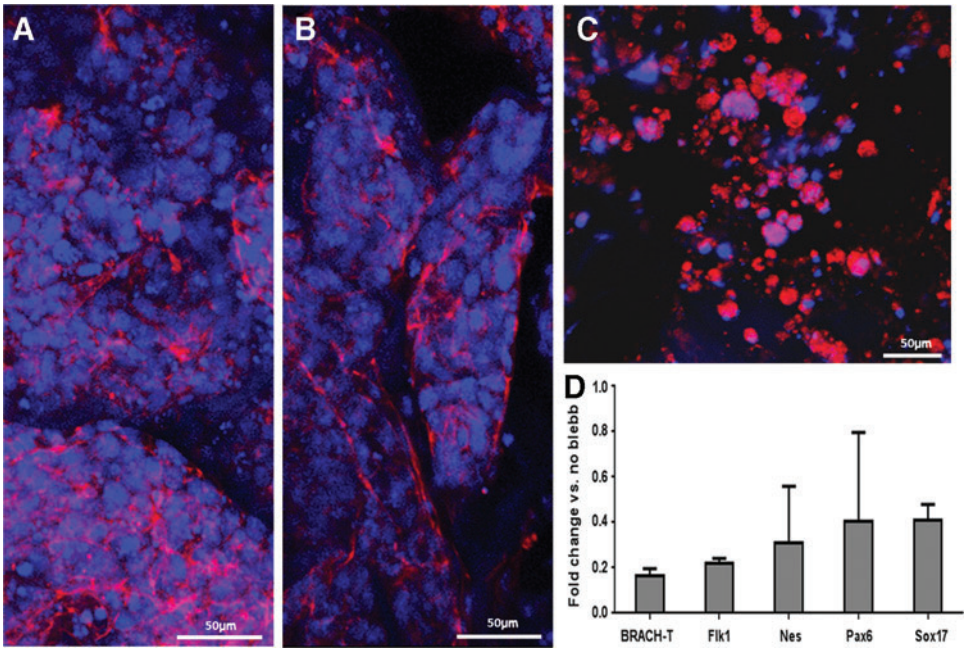

FIG. 6. Inhibition of myosin II led to massive downregulation of gene expression. Whole-mount actin fiber staining with phalloidin after a 6-day exposure to **(A)** control, **(B)** cyclic stretching, or **(C)** cyclic stretching in the presence of blebbistatin. **(D)** Real-time PCR analysis of genes representative of each of the three germ layers after exposure to cyclic stretching, in the presence of blebbistatin. Data are presented as percent change in gene expression when compared with cyclic stretching in the absence of blebbistatin as means ± standard error. Color images available online at www.liebertpub.com/tea

Discussion

In this study, we show that mechanical forces applied on mESCs within 3D environments can influence their fate. Under oscillatory stretching of whole 3D cell-embedded constructs, mESCs were directed toward differentiation into the mesoderm layer. Inhibition of nonmuscle myosin II, and subsequent prevention of submission of the mechanical cues, led to a significant decrease in *BRACH-T* and *Flk1* expression when compared to oscillatory stretching only.

Lack of an in-depth understanding of the factors controlling and influencing cell differentiation poses a major challenge in leveraging the vast clinical potential of ESCs. More comprehensive knowledge would enable exploitation of ESCs in therapeutic applications and large-scale differentiation techniques. To date, most studies have focused on the chemical and biological factors that can direct differentiation.[35,36] Little attention has been given to elucidation of the involvement of mechanical forces in the various differentiation stages, and of the degree to which they can assist in directing cells toward specific lineages or even in prompting them to further differentiate into a specific cell type. This study focused on characterizing the impact of mechanical cues on mESC differentiation, with emphasis on the early stages of differentiation into the mesoderm, ectoderm, and endoderm layers.

A 3D culture system was chosen to support mESC growth and differentiation within an environment similar to that of the embryo. In addition, this 3D environment encouraged the cells to form EBs within the scaffold pores, as demonstrated by the SEM images and H&E staining. Several studies that assess cell–matrix adhesion,[37] cancer cell interactions,[38] and cell differentiation[15,39] have demonstrated that cells behave differently in two-dimensional (2D) versus 3D environments. Human ESCs in 2D culture exposed to cyclic strains underwent inhibited cell differentiation,[40] contrasting our findings in a 3D environment. This emphasizes the important consideration of the 3D natural environment of the cells.

A commercial collagen scaffold was chosen due to its viscoelastic behavior and biological properties that closely mimic the natural environment of the cells within the body. In addition, collagen is one of the proteins in the ECM and was identified in the blastocyst inner cell mass.[41] Stretch force parameters were chosen according to previous studies and our preliminary observations. The selected frequency for cyclic stretch experiments was previously demonstrated by Chowdhury et al. who reported that local cyclic stress at 0.3 Hz applied on mESCs induced cell differentiation as manifested by downregulation in oct3/4 expression.[42] In addition, 30% strain amplitude was the initial part of the linear region of the stress–strain curve, in our setup (Fig. 2B, C), estimated as a stiffness of 21 kPa. Moreover, the 6-day postseeding time point was chosen following earlier observations of altered gene expression at this time point, in mESCs grown on substrates with different elasticities.[22]

Upon oscillatory stretching of the entire 3D construct, mESCs preferred mesodermal differentiation, which was inhibited by addition of blebbistatin. Real-time PCR analysis was performed to assess changes in gene expression resulting from the applied forces. Several studies that focus on changes in gene expression of ESCs chose the same genes as representative of each germ layer.[22,26] Other studies also chose *BRACH-T* as representative of the mesoderm germ layer and indicated change in cell differentiation based on its expression. For example, shear stress was shown to induce mESC differentiation, where changes in magnitude and duration of the applied stress resulted in changes in gene expression for the ectoderm and mesoderm germ layers.[27]

Analysis of gene expression, using a microfluidic TaqMan array, following a 6-day cyclic stretching regimen identified a group of mesodermal genes that were influenced by the manipulation, and were attributed to biological processes associated with muscle and cardiovascular development. The changes observed in expression of genes related

to pluripotency and stemness (Fig. 5B) further indicated initiation of differentiation and viability tests (presented in Supplementary Fig. S4) demonstrated a high percentage of viability under the applied forces. Taken together, these findings suggest that the cells are growing and differentiating under the applied forces, which direct them toward mesodermal fate.

ESC development and differentiation are complex processes, which begin with the gastrulation stage, characterized by a biomechanical process that transforms a group of cells into the embryo, an organized 3D sphere of cells. Forces along with cell movement play key regulatory roles in this, suggesting that their external application in culture, in the form of compression, tension, and shear stresses, can induce the same processes.[43] The mesoderm and endoderm cells move to inside the sphere toward the definitive endoderm layer, whereas the ectoderm cells are located on the surface.[16] Our results show that genes representative of the endoderm and mesoderm are more influenced than those associated with the ectoderm. This may be explained by the more intense mechanical forces experienced by the inner cells within the sphere when compared with the outer cells. Upregulation in some mesoderm representative genes suggests that mechanical forces trigger the differentiation toward the mesoderm, while most of the endoderm-related genes are downregulated. Gene expression analysis indicated upregulation of mesodermal processes, such as vasculogenesis, development of cardiovascular tissue, differentiation of endothelial cells, embryo morphogenesis, and other processes, such as cell proliferation, movement, migration, differentiation, and morphology. As the endoderm and mesoderm cells are grouped together, we can assume that during embryogenesis, the cells that experience higher mechanical forces are directed to the mesoderm germ layer and not to the endoderm.

The method used in this study for examining the correlation between mechanical forces and ESC differentiation overcomes limitations of other approaches, in that it allows application of mechanical forces within the same 3D structures without modifying the overall environment. Consequently, this setup enables evaluation of the pure influence of external force on the cells. Moreover, the scaffold used in this study demonstrated viscoelastic properties characterized by the nonlinear stress–strain curve and the hysteresis loop in the stress–strain curve of one cycle in the cyclic stretching protocol. The observed viscoelastic behavior of the scaffold mimics tissue properties, demonstrating close resemblance of the scaffold to natural environments, along with the capability of the scaffold to resist the external forces and to stretch to high strain values, maintained also after cell seeding (Fig. 2C).

Additionally, although only two mechanical manipulation regimens were assessed in this study, the resulting lineage commitment demonstrated differential sensitivity to the mechanical cues. However, at the same time, no differences were noted in cell responses to static force, which may have been the result of inevitable transmission of static forces on one side of the scaffold in the control setup. Among all the examined mechanical conditions, oscillatory forces had the greatest influence on cell differentiation. This phenomenon has been also observed for other cells; for example, mesenchymal stem cells that have been shown to be influenced by external mechanical signals,[44] where, for example, cyclic compressive strain alone induced osteogenic lineage commitment.[45]

Undifferentiated ESCs have been shown to be softer, as defined by the ratio of the strain to the applied stress, when compared with their differentiated state, rendering them more susceptible to the effects of local cyclic forces.[42] This report resonates with our present results, which demonstrated a greater influence of cyclic stretching on undifferentiated cells, when compared with cells that were first differentiated in the form of EBs. In addition, application of cyclic stretching led to loss of stemness. Similar findings have been reported for mesenchymal stem cells under the influence of external factors, such as diverse matrix stiffness and applied mechanical strain.[46]

In efforts to determine whether the underlying biophysical mechanism for ESC differentiation is governed by cytoskeletal deformation, we quantified gene expression after applying oscillatory forces, in the presence of the myosin II ATPase inhibitor blebbistatin.[47] Blebbistatin influences cell blebbing during cell division, resulting in a decrease in the steady-state actin-activated ATPase activity of nonmuscle myosin II.[48] Cyclic stretching in the presence of blebbistatin resulted in downregulation of cell differentiation, when compared with cyclic stretching, where the greatest influence was observed in the expression of *BRACH-T* and *Flk1*, further demonstrating the role of cytoskeletal elements on mesodermal differentiation. Upon cell adherence to the ECM, a continuous link between the cell cytoskeleton and ECM is created, forming a means of direct transmission of mechanical signal to the cell and resulting in elastic tension in the cell cytoskeleton. This elastic tension is maintained by myosin II molecular motors, which apply contractile forces on the actin filaments, resulting in compression of the cytoskeleton.[3] These elastic stresses regulate processes within the cell, including, as suggested by our results, early stages of differentiation of the embryo. Additionally, upon inhibition of myosin II, we recorded downregulation of mesodermal genes, suggesting that the mesoderm germ layer is most affected by external forces, under the conditions applied in this study. After cyclic stretching, actin fibers were spread and aligned in the direction of the stretching. However, inhibition of myosin II activity resulted in rounded cell that failed to spread within the matrix. These findings lie in agreement with those that have demonstrated the significant role of myosin II in regulation of cell organization in the first days of the mouse embryo, where its deficiency led to absence of germ layer organization.[49]

In conclusion, our results show, for the first time, that early differentiation of ESCs is sensitive to tensile forces. Moreover, this experimental setup demonstrates the ability to manipulate and examine ESC differentiation and other processes occurring within 3D natural-mimic constructs. While other studies rely on 2D substrates or manipulation of the mechanical properties of the matrix, this work integrated a 3D environment with external tensile mechanical forces.

Acknowledgments

The authors would like to thank Grigori Enikolopov for Nestin-GFP mESC gift. This research was funded by the ERC grant ENGVASC and NanoCARD grant (grant agreement No.

229294) of the European Union 7th Framework Program and the Israel Science Foundation. We would also like to thank the Russell Berrie Nanotechnology Institute at the Technion and the Ed Sattel scholarship (D.D.-R.) for their support. We would also like to thank Michael Shmoish for his help with microfluidic card gene analysis, Tslil Biton and Prof. Michael S. Silverstein for helping with the SEM imaging, Jennette Zavin for her help with stem cell growth, and Yehudit Posen for article editing.

Disclosure Statement

No competing financial interests exist.

References

1. Odorico, J.S., Kaufman, D.S., and Thomson, J.A. Multilineage differentiation from human embryonic stem cell lines. Stem Cells **19,** 193, 2001.
2. Amit, M., and Itskovitz-Eldor, J. Derivation and spontaneous differentiation of human embryonic stem cells. J Anat **200,** 225, 2002.
3. Dado, D., Sagi, M., Levenberg, S., and Zemel, A. Mechanical control of stem cell differentiation. Regen Med **7,** 101, 2012.
4. Dang, S.M., Gerecht-Nir, S., Chen, J., Itskovitz-Eldor, J., and Zandstra, P.W. Controlled, scalable embryonic stem cell differentiation culture. Stem Cells **22,** 275, 2004.
5. Peerani, R., Rao, B.M., Bauwens, C., Yin, T., Wood, G.A., Nagy, A., Kumacheva, E., and Zandstra, P.W. Niche-mediated control of human embryonic stem cell self-renewal and differentiation. EMBO J **26,** 4744, 2007.
6. Suri, S., Singh, A., Nguyen, A.H., Bratt-Leal, A.M., McDevitt, T.C., and Lu, H. Microfluidic-based patterning of embryonic stem cells for *in vitro* development studies. Lab Chip **13,** 4617, 2013.
7. Khoury, M., Bransky, A., Korin, N., Konak, L.C., Enikolopov, G., Tzchori, I., and Levenberg, S. A microfluidic traps system supporting prolonged culture of human embryonic stem cells aggregates. Biomed Microdevices **12,** 1001, 2010.
8. Levenberg, S., Huang, N.F., Lavik, E., Rogers, A.B., Itskovitz-Eldor, J., and Langer, R. Differentiation of human embryonic stem cells on three-dimensional polymer scaffolds. Proc Natl Acad Sci U S A **100,** 12741, 2003.
9. Goh, S.K., Olsen, P., and Banerjee, I. Extracellular matrix aggregates from differentiating embryoid bodies as a scaffold to support ESC proliferation and differentiation. PLoS One **8,** e61856, 2013.
10. Lee, S.T., Yun, J.I., van der Vlies, A.J., Kontos, S., Jang, M., Gong, S.P., Kim, D.Y., Lim, J.M., and Hubbell, J.A. Long-term maintenance of mouse embryonic stem cell pluripotency by manipulating integrin signaling within 3D scaffolds without active Stat3. Biomaterials **33,** 8934, 2012.
11. Tzezana, R., Reznik, S., Blumenthal, J., Zussman, E., and Levenberg, S. Regulation of stem cell differentiation by control of retinoic acid gradients in hydrospun 3D scaffold. Macromol Biosci **12,** 598, 2012.
12. Bratt-Leal, A.M., Carpenedo, R.L., Ungrin, M.D., Zandstra, P.W., and McDevitt, T.C. Incorporation of biomaterials in multicellular aggregates modulates pluripotent stem cell differentiation. Biomaterials **32,** 48, 2011.
13. Gerecht, S., Burdick, J.A., Ferreira, L.S., Townsend, S.A., Langer, R., and Vunjak-Novakovic, G. Hyaluronic acid hydrogel for controlled self-renewal and differentiation of human embryonic stem cells. Proc Natl Acad Sci U S A **104,** 11298, 2007.
14. Dang, S.M., Kyba, M., Perlingeiro, R., Daley, G.Q., and Zandstra, P.W. Efficiency of embryoid body formation and hematopoietic development from embryonic stem cells in different culture systems. Biotechnol Bioeng **78,** 442, 2002.
15. Pineda, E.T., Nerem, R.M., and Ahsan, T. Differentiation patterns of embryonic stem cells in two- versus three-dimensional culture. Cells Tissues Organs **197,** 399, 2013.
16. Murry, C.E., and Keller, G. Differentiation of embryonic stem cells to clinically relevant populations: lessons from embryonic development. Cell **132,** 661, 2008.
17. Nowotschin, S., and Hadjantonakis, A.-K. Cellular dynamics in the early mouse embryo: from axis formation to gastrulation. Curr Opin Genet Dev **20,** 420, 2010.
18. Arnold, S.J., and Robertson, E.J. Making a commitment: cell lineage allocation and axis patterning in the early mouse embryo. Nat Rev Mol Cell Biol **10,** 91, 2009.
19. Gadue, P., Huber, T.L., Nostro, M.C., Kattman, S., and Keller, G.M. Germ layer induction from embryonic stem cells. Exp Hematol **33,** 955, 2005.
20. Leung, M.C., Cooper, A., Jana, S., Tsao, C.-T., Petrie, T., and Zhang, M. Nanofiber-based *in vitro* system for high myogenic differentiation of human embryonic stem cells. Biomacromolecules **14,** 4207, 2013.
21. Engler, A.J., Sen, S., Sweeney, H.L., and Discher, D.E. Matrix elasticity directs stem cell lineage specification. Cell **126,** 677, 2006.
22. Evans, N.D., Minelli, C., Gentleman, E., LaPointe, V., Patankar, S.N., Kallivretaki, M., Chen, X., Roberts, C.J., and Stevens, M.M. Substrate stiffness affects early differentiation events in embryonic stem cells. Eur Cell Mater **18,** 1, 2009.
23. Chowdhury, F., Li, Y., Poh, Y.C., Yokohama-Tamaki, T., Wang, N., and Tanaka, T.S. Soft substrates promote homogeneous self-renewal of embryonic stem cells via downregulating cell-matrix tractions. PLoS One **5,** e15655, 2010.
24. McBeath, R., Pirone, D.M., Nelson, C.M., Bhadriraju, K., and Chen, C.S. Cell shape, cytoskeletal tension, and RhoA regulate stem cell lineage commitment. Dev Cell **6,** 483, 2004.
25. Kilian, K.A., Bugarija, B., Lahn, B.T., and Mrksich, M. Geometric cues for directing the differentiation of mesenchymal stem cells. Proc Natl Acad Sci U S A **107,** 4872, 2010.
26. Zoldan, J., Karagiannis, E.D., Lee, C.Y., Anderson, D.G., Langer, R., and Levenberg, S. The influence of scaffold elasticity on germ layer specification of human embryonic stem cells. Biomaterials **32,** 9612, 2011.
27. Wolfe, R.P., Leleux, J., Nerem, R.M., and Ahsan, T. Effects of shear stress on germ lineage specification of embryonic stem cells. Integr Biol (Camb) **4,** 1263, 2012.
28. Wolfe, R.P., and Ahsan, T. Shear stress during early embryonic stem cell differentiation promotes hematopoietic and endothelial phenotypes. Biotechnol Bioeng **110,** 1231, 2013.
29. Gleiberman, A.S., Encinas, J.M., Mignone, J.L., Michurina, T., Rosenfeld, M.G., and Enikolopov, G. Expression of nestin-green fluorescent protein transgene marks oval cells in the adult liver. Dev Dyn **234,** 413, 2005.
30. Takeuchi, J.K., and Bruneau, B.G. Directed transdifferentiation of mouse mesoderm to heart tissue by defined factors. Nature **459,** 708, 2009.

31. Ku, C.H., Johnson, P.H., Batten, P., Sarathchandra, P., Chambers, R.C., Taylor, P.M., Yacoub, M.H., and Chester, A.H. Collagen synthesis by mesenchymal stem cells and aortic valve interstitial cells in response to mechanical stretch. Cardiovasc Res **71,** 548, 2006.
32. Lin, C.Y., Lee, H.C., Chen, H.C., Hsieh, C.C., and Tsai, H.J. Normal function of Myf5 during gastrulation is required for pharyngeal arch cartilage development in zebrafish embryos. Zebrafish **10,** 486, 2013.
33. Zajac, A.L., and Discher, D.E. Cell differentiation through tissue elasticity-coupled, myosin-driven remodeling. Curr Opin Cell Biol **20,** 609, 2008.
34. Even-Ram, S., Doyle, A.D., Conti, M.A., Matsumoto, K., Adelstein, R.S., and Yamada, K.M. Myosin IIA regulates cell motility and actomyosin-microtubule crosstalk. Nat Cell Biol **9,** 299, 2007.
35. Takahashi, K., Tanabe, K., Ohnuki, M., Narita, M., Ichisaka, T., Tomoda, K., and Yamanaka, S. Induction of pluripotent stem cells from adult human fibroblasts by defined factors. Cell **131,** 861, 2007.
36. Bratt-Leal, A.M., Carpenedo, R.L., and McDevitt, T.C. Engineering the embryoid body microenvironment to direct embryonic stem cell differentiation. Biotechnol Prog **25,** 43, 2009.
37. Cukierman, E., Pankov, R., Stevens, D.R., and Yamada, K.M. Taking cell-matrix adhesions to the third dimension. Science **294,** 1708, 2001.
38. Krishnan, V., Shuman, L.A., Sosnoski, D.M., Dhurjati, R., Vogler, E.A., and Mastro, A.M. Dynamic interaction between breast cancer cells and osteoblastic tissue: comparison of two- and three-dimensional cultures. J Cell Physiol **226,** 2150, 2011.
39. Caron, M.M.J., Emans, P.J., Coolsen, M.M.E., Voss, L., Surtel, D.A.M., Cremers, A., van Rhijn, L.W., and Welting, T.J.M. Redifferentiation of dedifferentiated human articular chondrocytes: comparison of 2D and 3D cultures. Osteoarthritis Cartilage **20,** 1170, 2012.
40. Saha, S., Ji, L., de Pablo, J.J., and Palecek, S.P. Inhibition of human embryonic stem cell differentiation by mechanical strain. J Cell Physiol **206,** 126, 2006.
41. Kraehenbuehl, T.P., Langer, R., and Ferreira, L.S. Three-dimensional biomaterials for the study of human pluripotent stem cells. Nat Methods **8,** 731, 2011.
42. Chowdhury, F., Na, S., Li, D., Poh, Y.C., Tanaka, T.S., Wang, F., and Wang, N. Material properties of the cell dictate stress-induced spreading and differentiation in embryonic stem cells. Nat Mater **9,** 82, 2010.
43. Keller, R., Davidson, L.A., and Shook, D.R. How we are shaped: the biomechanics of gastrulation. Differentiation **71,** 171, 2003.
44. Kelly, D.J., and Jacobs, C.R. The role of mechanical signals in regulating chondrogenesis and osteogenesis of mesenchymal stem cells. Birth Defects Res C Embryo Today **90,** 75, 2010.
45. Michalopoulos, E., Knight, R.L., Korossis, S., Kearney, J.N., Fisher, J., and Ingham, E. Development of methods for studying the differentiation of human mesenchymal stem cells under cyclic compressive strain. Tissue Eng Part C Methods **18,** 252, 2012.
46. Kuhn, N.Z., and Tuan, R.S. Regulation of stemness and stem cell niche of mesenchymal stem cells: implications in tumorigenesis and metastasis. J Cell Physiol **222,** 268, 2010.
47. Kovacs, M., Toth, J., Hetenyi, C., Malnasi-Csizmadia, A., and Sellers, J.R. Mechanism of blebbistatin inhibition of myosin II. J Biol Chem **279,** 35557, 2004.
48. Ramamurthy, B., Yengo, C.M., Straight, A.F., Mitchison, T.J., and Sweeney, H.L. Kinetic mechanism of blebbistatin inhibition of nonmuscle myosin IIb. Biochemistry **43,** 14832, 2004.
49. Conti, M.A., Even-Ram, S., Liu, C., Yamada, K.M., and Adelstein, R.S. Defects in cell adhesion and the visceral endoderm following ablation of nonmuscle myosin heavy chain II-A in mice. J Biol Chem **279,** 41263, 2004.

Address correspondence to:
Shulamit Levenberg, PhD
Department of Biomedical Engineering
Technion–Israel Institute of Technology
Haifa 32000
Israel

E-mail: shulamit@bm.technion.ac.il

Received: January 6, 2014
Accepted: June 25, 2014
Online Publication Date: August 6, 2014